

N⁶-Methyladenosine Modification of Fatty Acid Amide Hydrolase Messenger RNA in Circular RNA STAG1-Regulated Astrocyte Dysfunction and Depressive-like Behaviors

Rongrong Huang, Yuan Zhang, Ying Bai, Bing Han, Minzi Ju, Biling Chen, Li Yang, Yu Wang, Hongxing Zhang, Haisan Zhang, Chunming Xie, Zhijun Zhang, and Honghong Yao

ABSTRACT

BACKGROUND: N⁶-methyladenosine (m⁶A) is the most abundant epigenetic modification in eukaryotic messenger RNAs and is essential for multiple RNA processing events in physiological and pathological processes. However, precisely how m⁶A methylation is involved in major depressive disorder (MDD) is not fully understood.

METHODS: Circular RNA STAG1 (circSTAG1) was screened from the hippocampus of chronic unpredictable stress-treated mice using high-throughput RNA sequencing. Microinjection of circSTAG1 lentivirus into the mouse hippocampus was used to observe the role of circSTAG1 in depression. Sucrose preference, forced swim, and tail suspension tests were performed to evaluate the depressive-like behaviors of mice. Astrocyte dysfunction was examined by GFAP immunostaining and 3D reconstruction. Methylated RNA immunoprecipitation sequence analysis was used to identify downstream targets of circSTAG1/ALKBH5 (alkB homolog 5) axis. Cell Counting Kit-8 assay was performed to evaluate astrocyte viability *in vitro*.

RESULTS: circSTAG1 was significantly decreased in the chronic unpredictable stress-treated mouse hippocampus and in peripheral blood of patients with MDD. Overexpression of circSTAG1 notably attenuated astrocyte dysfunction and depressive-like behaviors induced by chronic unpredictable stress. Further examination indicated that overexpressed circSTAG1 captured ALKBH5 and decreased the translocation of ALKBH5 into the nucleus, leading to increased m⁶A methylation of fatty acid amide hydrolase (FAAH) messenger RNA and degradation of FAAH in astrocytes with subsequent attenuation of depressive-like behaviors and astrocyte loss induced by corticosterone *in vitro*.

CONCLUSIONS: Our findings dissect the functional link between circSTAG1 and m⁶A methylation in the context of MDD, providing evidence that circSTAG1 may be a novel therapeutic target for MDD.

Keywords: ALKBH5, Astrocyte, circSTAG1, Depression, FAAH, N⁶-methyladenosine

<https://doi.org/10.1016/j.biopsych.2020.02.018>

Major depressive disorder (MDD) is one of the most common psychiatric disorders around the world; characterized by emotional dysfunction, it is an important public health concern with serious consequences (1–4). Approximately 350 million people worldwide experience MDD, and 15% of the patients with MDD have a history of attempted suicide (5). The mechanism of MDD is complex, and its occurrence and development result from a combination of environmental and genetic factors (6), with stress as a serious risk factor (7,8). Current diagnostic techniques do not fully reflect MDD's dynamic physiological and biochemical indices and neurobiological alterations (5,9). In addition, effective antidepressant drugs are lacking, and nearly one third of patients with MDD do not respond adequately to current drugs (10,11). Further investigation of the detailed mechanisms of MDD is beneficial to identify more effective therapeutic targets.

Circular RNAs (circRNAs) are a class of RNAs in the eukaryotic transcriptome. They use covalent linkage of the ends to form a circular structure without the 5' and 3' ends (12,13). Most circRNAs are composed of exon sequences of protein-coding genes and are highly conserved in different species, although some are also derived from intronic, intergenic, and untranslated regions. Recent studies showed that circRNAs expressing in the cytoplasm of mammal cells could act as microRNA (miRNA) sponges to block the effect of miRNA on target messenger RNA (mRNA) and regulate disease processes such as depression, stroke, and cancer (14–16). Our previous studies showed that circDYM ameliorates depressive-like behaviors by targeting miR-9 to regulate microglial activation via HSP90 ubiquitination (15), indicating that circRNAs are involved in depression. Encouraged by this finding, we explored the roles of other circRNAs in depression

SEE COMMENTARY ON PAGE 362

using high-throughput sequencing and found that circRNA-mm9_circ_0015149, known as circSTAG1, was down-regulated in chronic unpredictable stress (CUS)-treated mice (GEO accession number: GSE135343). However, the function and explicit downstream mechanisms underlying circSTAG1 remain unclear.

Accumulating evidence indicates that N⁶-methyladenosine (m⁶A) is the most common posttranscriptional internal mRNA modification, especially in the 3'-UTR (untranslated region) near the translation termination codon. RNA m⁶A modification is catalyzed by a methyltransferase complex comprising METTL3 (methyltransferase-like 3), METTL14 (methyltransferase-like 14), and WRAP (Wilms tumor 1 associated protein). RNA demethylation is catalyzed by two m⁶A demethylases: FTO (fat mass and obesity-associated protein) and ALKBH5 (alkB homolog 5). In response to different signals during normal physical processes or under diseases, m⁶A markers are dynamically installed and removed from their regulated transcripts to regulate RNA metabolisms, including mRNA splicing, nuclear export, translation, and miRNA processing. A previous study indicated that brain m⁶A methylation exhibits a novel layer of complexity in gene expression regulation after stress, and stress-related psychiatric disorder may arise from dysfunction of m⁶A response (17). Growing evidence demonstrates that both FTO genetic variants and ALKBH5 are associated with MDD (18,19). Consistent with these aforementioned findings, our current study indicates that there is significant decrease of m⁶A in CUS mice. However, whether there is a functional link between downregulated circSTAG1 and m⁶A RNA modulation in the context of MDD remains unknown.

Astrocyte dysfunction has been found to play a key role in depression (20,21). Growing evidence also shows an association between astrocytes and DNA methylation in depression (22). In the prefrontal cortex of patients with MDD who died during a depressive episode, astrocyte-related genes displayed reduced methylation (22). CUS mice also exhibit long-term demethylation in the *Crf* gene, while site-specific knockdown of the *Crf* gene to reduce demethylation attenuated stress-induced depressive-like behaviors (23). However, whether RNA m⁶A methylation affects astrocyte function is largely unknown.

In this study, we dissected the correlation of circSTAG1 and m⁶A methylation with MDD. We discovered a crucial effect of circSTAG1 in attenuating depressive-like behaviors and confirmed m⁶A methylation as an important downstream mechanism pathway of circSTAG1. circSTAG1 overexpression captured ALKBH5 and decreased the translocation of ALKBH5 into the nucleus, leading to increased m⁶A methylation of fatty acid amide hydrolase (FAAH) mRNA and degradation of FAAH in astrocytes with subsequent attenuation of depressive-like behaviors and astrocyte loss induced by corticosterone in vitro. Our findings enrich the current literature on the functional link between circSTAG1 and m⁶A methylation in the context of MDD, providing evidence that circSTAG1 may be a novel therapeutic target for MDD.

METHODS AND MATERIALS

Study Approval and Human Subjects

This research protocol was approved by the ethics committee at Henan Provincial Mental Hospital, affiliated with Xinxiang

Medical University (approval ID: 2017-08). Participants or their legally authorized representatives provided written informed consent. Patients with MDD were enlisted from the Department of Psychiatry at Henan Provincial Mental Hospital. Healthy control subjects were recruited through media advertising and local community posting.

Animals

Male C57BL/6J mice (6-8 weeks old) were purchased from the Model Animal Research Center of Nanjing University. More details are provided in the [Supplement](#).

CUS Procedure

According to the procedure previously validated in mice (24,25), the CUS protocol applied in this study was performed with some modifications. Mice were exposed to several random kinds of stress, one or two kinds of low-intensity social-environmental stressors, each day for 4 weeks. The stressors applied in this study are described in the [Supplement](#).

Lentivirus Microinjection

The circSTAG1 and ALKBH5 short hairpin RNA (shRNA) lentivirus (1.5 μ L, 10⁹ viral genomes/ μ L) (HanBio, Shanghai, China) was microinjected into the hippocampus of C57BL/6J mice bilaterally using the following microinjection coordinates: 2.0 mm behind the bregma and \pm 1.5 mm lateral from the sagittal midline at a depth of 2 mm below the skull surface.

Luciferase Activity Assays

Primary astrocytes were seeded in 96-well plates and transfected with pMIR-REPORT luciferase vector with wild-type or mutated FAAH 3'-UTR (RiboBio, Guangzhou, China) for 24 hours. Reporter assays were performed following the manufacturer's protocol (E2920; Promega, Madison, WI). Renilla luciferase activity was normalized to a firefly luciferase signal and quantified as a percentage of the control.

Measurement of Total m⁶A

Total m⁶A modification level was measured in 200 ng RNA extracted from the mouse hippocampus. m⁶A levels of total RNA were measured using an m⁶A RNA methylation quantification kit (P-9005; EpiGentek, Farmingdale, NY) according to the manufacturer's instructions.

Western Blotting and Other Experiments

Western blotting, Cell Counting Kit-8 assay, real-time polymerase chain reaction (PCR), fluorescence in situ hybridization, flow cytometry analysis, immunostaining, and image analysis were performed as described in the [Supplement](#).

Statistical Analysis

Statistical analysis was performed using GraphPad Prism 7 (GraphPad Software, San Diego, CA). Significance was assessed using Student's *t* test for comparisons of two groups. One-way ANOVA followed by the Holm-Sidak test and two-way analysis of variance followed by Bonferroni's post hoc multiple comparison tests was used for multigroup comparison. All data are presented as mean \pm SEM. The statistical

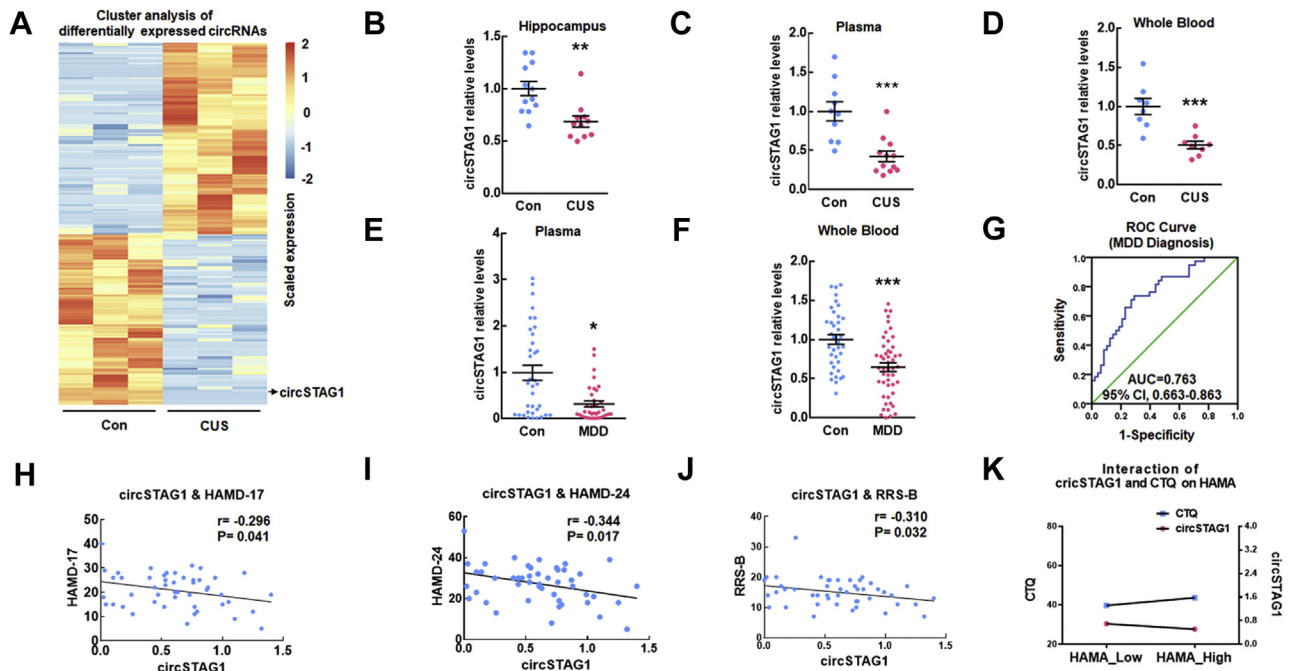


Figure 1. circSTAG1 was downregulated in CUS mice and patients with MDD. **(A)** Distinct circRNA expression in CUS mouse hippocampus tissues compared with that in control tissues (fold change ≥ 1.5 , $p < .05$). **(B)** Levels of circSTAG1 were decreased in the hippocampus tissues of CUS mice ($n = 10$) compared with the control group ($n = 10$), $t_{21} = 3.587$. **(C)** Levels of circSTAG1 were decreased in the plasma of CUS mice ($n = 12$) compared with the control group ($n = 10$), $t_{20} = 4.322$. **(D)** Levels of circSTAG1 were decreased in the whole blood of CUS mice ($n = 8$) compared with the control group ($n = 8$), $t_{14} = 4.334$. **(E)** Levels of circSTAG1 were decreased in the plasma of patients with MDD ($n = 35$) compared with healthy control subjects ($n = 35$), $t_{68} = 3.836$. **(F)** Levels of circSTAG1 were decreased in the whole blood of patients with MDD ($n = 38$) compared with healthy control subjects ($n = 47$), $t_{85} = 4.261$. **(G)** ROC curve for individual circSTAG1 to separate patients with MDD from healthy control subjects. **(H)** Correlation between circSTAG1 expression and HAMD-17 scores using Pearson's correlation coefficient. **(I)** Correlation between circSTAG1 expression and HAMD-24 scores using Pearson's correlation coefficient. **(J)** Correlation between circSTAG1 expression and RRS-B scores using Pearson's correlation coefficient. **(K)** Interactive effects of circSTAG1 and CTQ scores on HAMA scores in patients with MDD using multivariate linear regression. Patients with MDD with lower circSTAG1 and CTQ scores showed more severe depressive symptoms. All data are presented as mean \pm SEM. * $p < .05$, ** $p < .01$, and *** $p < .001$ vs. control groups. AUC, area under the curve; CI, confidence interval; circ, circular RNA; Con, control; CTQ, Childhood Trauma Questionnaire; CUS, chronic unpredictable stress; HAMA, Hamilton Anxiety Scale; HAMD-17, Hamilton Depression Scale-17 items; HAMD-24, Hamilton Depression Scale-24 items; MDD, major depressive disorder; ROC, receiver operating characteristic; RRS-B, Ruminative Responses Scale-Brooding.

analyses used for the different experiments are described in the respective figure legends, and results were considered significant at $p < .05$.

RESULTS

circSTAG1 Is Decreased in the CUS Mouse Hippocampus and Blood of Patients With MDD

To investigate the potential involvement of circRNAs in MDD, we isolated the hippocampus from the brains of depressive-like CUS mice and performed circRNA high-throughput sequencing. A heat map revealed that 217 circRNAs showed a differential expression in CUS samples compared with control samples (Figure 1A and Table S1). Among the 217 circRNAs, we identified 18 circRNAs with high homology between human and mouse (sequence similarity $>85\%$) in Table S2. These 18 circRNAs (10 upregulated and 8 downregulated) were further verified in the mouse hippocampus by real-time PCR. In the 10 upregulated circRNAs, none of the circRNAs was validated in the individual samples of hippocampus (Figure S1A). However, the

level of circDOCK4-1, circSTAG1, circKALRN, and circDOCK4-2 was consistent with circRNA sequencing among the 8 downregulated circRNAs (Figure S1B). Only circSTAG1 was able to be determined in the plasma of human and mouse (Figure S1C). Therefore, circSTAG1 was the focus in our current study for the potential role in MDD.

circSTAG1 (mm9_circ_0015149), a homologous human and mouse circRNA derived from exons 2, 3, 4, and 5 of the *STAG1* gene (Figure S2A), was further investigated for its potential role in depression. Head-to-tail junction-specific primers for circSTAG1 in real-time PCR analysis are presented in Figure S2B, C. Notably, circSTAG1 exhibited decreased expression in the CUS mouse hippocampus (Figure 1B), plasma (Figure 1C), and whole blood (Figure 1D) compared with the control group. In addition to the brain and blood, we verified the expression of circSTAG1 in other organs such as the heart, liver, spleen, lung, and kidney. circSTAG1 was highly expressed in the brain compared with other tissues, and there was no significant difference in the circSTAG1 expression of heart, liver, spleen, lung, and kidney between the control and CUS groups

(Figure S2D, E). There is no significant difference of STAG1 mRNA expression between the control and CUS groups (Figure S3A) or between the healthy and MDD groups (Figure S3B). RNase R resistance of circSTAG1 was quantified by real-time PCR with confirmed head-to-tail splicing, and endogenous circSTAG1 was strongly resistant to RNase R (Figure S4A). RNA extracted from H293T cells transfected with circSTAG1 plasmid was amplified with circSTAG1 primers (Figure S4B), and the sequence of splicing site was confirmed by sequencing, as shown in Figure S4C. Exogenous circSTAG1 showed at least 10-fold more resistance to RNase R than GAPDH (Figure S4D).

To determine whether circSTAG1 is involved in depression, we examined circSTAG1 levels in healthy control subjects and patients with MDD. The demographic and clinical characteristics of these subjects are listed in Tables S3 to S5. Further analysis of clinical samples showed that circSTAG1 was significantly decreased in the plasma and whole blood of patients with depression compared with those of gender- and age-matched normal control subjects (Figure 1E, F). The analysis of receiver operating characteristic curve revealed that circSTAG1 exhibited a significant area under the curve of 0.763 with 0.711 sensitivity and 0.694 specificity (Figure 1G). Moreover, as shown in Figure 1H–J, there was a negative correlation between circSTAG1 levels and the scores of Hamilton Depression Scale (HAMD)-17 items (Pearson correlation coefficient $r = -.296$, $p = .041$), between circSTAG1 levels and the scores of HAMD-24 items (Pearson correlation coefficient $r = -.344$, $p = .017$), and between circSTAG1 levels and the scores of Ruminative Responses Scale–Brooding (Pearson correlation coefficient $r = -.310$, $p = .032$). Linear regression analysis revealed that patients with MDD who had lower expression of circSTAG1 and higher Childhood Trauma Questionnaire scores showed more severe depressive symptoms (Figure 1K).

Overexpression of circSTAG1 Ameliorates Depressive-like Behaviors Induced by CUS

We next sought to investigate the effect of circSTAG1 on CUS mice by microinjecting either the circControl-GFP or circSTAG1-GFP lentivirus into the mouse hippocampus as illustrated in Figure 2A, B. Two weeks later, green fluorescent protein (GFP) lentivirus expression was largely restricted to the whole hippocampus (Figure 2C and Figure S5A), and circSTAG1 expression was significantly upregulated in the hippocampus (Figure S5B). Neurons, astrocytes, and microglia cells were colocalized with GFP signal in the hippocampus (Figure S5C). The expression of circSTAG1 was significantly decreased in the CUS treatment group compared with the control group and was ameliorated by circSTAG1 overexpression (Figure 2D). For depressive-like behaviors, CUS treatment decreased sucrose preference compared with the control group; the deficit was notably rescued by circSTAG1 overexpression (Figure 2E). The forced swim test and the tail suspension test were also performed to evaluate the antidepressant effect of circSTAG1. As shown in Figure 2F (forced swim test) and Figure 2G (tail suspension test), microinjection of circSTAG1 significantly inhibited the increase of immobility induced by CUS. Moreover, the behavioral test did not exert a significant effect on the circSTAG1 expression (Figure S6).

Overexpression of circSTAG1 Attenuates Astrocyte Dysfunction in the CUS Mouse Hippocampus

To further assess which cells that derived circSTAG1 are downregulated in the depressive-like brain, we compared circSTAG1 levels in the cell lysates of neurons (NCAM-1⁺), astrocytes (ACSA-2⁺), and microglia cells (CD11b⁺CD45^{dim}) isolated from the CUS model (Figure 3A). We found that astrocyte-derived circSTAG1 was significantly downregulated compared with that derived from microglia cells or neurons (Figure 3B). There was not cell type-specific expression of circSTAG1 and linear STAG1 transcript in astrocytes, neurons, and microglia cells (Figure S7). In situ hybridization was performed to further confirm the expression of circSTAG1 in astrocytes (Figure 3C), and circSTAG1 was found mainly distributed in the astrocyte cytoplasm (Figure S8).

Because CUS mice experience neuroinflammation leading to astrocyte dysfunction (26,27), we next sought to examine circSTAG1's effect on astrocyte function. As shown in Figure 3D, the expression of GFAP, which is a marker of astrocytes, notably decreased in the hippocampus of CUS mice; this was rescued by circSTAG1 overexpression. This finding was confirmed by GFAP staining (Figure 3E). CUS exposure resulted in astrocyte dysfunction in circControl mice, as indicated by the fact that CUS exposure decreased the number of GFAP-positive cells (Figure 3F) and by the ramification of astrocytes, as characterized by significantly decreased branch length, volume, and numbers (Figure 3G–I).

circSTAG1 Binds With ALKBH5 in the Astrocyte Cytoplasm

Given m⁶A methylation's potential involvement in MDD (17,19), we next sought to examine total m⁶A methylation in the CUS model. As shown in Figure 4A, CUS treatment decreased m⁶A in total hippocampus RNA, which was significantly attenuated by circSTAG1 overexpression, indicating a functional link between circSTAG1 and m⁶A methylation. circSTAG1 overexpression in astrocytes increased the m⁶A level in total RNA, and circSTAG1 small interfering RNA (siRNA) decreased the m⁶A level in total RNA (Figure S9A, B). Further experiments showed that circSTAG1 did not affect the expression of m⁶A RNA methylases (METTL3, METTL14, and WTAP) or demethylases (FTO and ALKBH5) (Figures S10 and S11). These findings prompted us to speculate that there is interaction between circSTAG1 and m⁶A RNA methylases or demethylases. Thus, RNA immunoprecipitation assay was performed to determine the interaction between circSTAG1 and m⁶A RNA methylases or demethylases. As shown in Figure 4B, circSTAG1, but not STAG1 mRNA, showed a stronger affinity to ALKBH5 than the negative control circHECW2 and GAPDH. However, circSTAG1 barely adsorbed FTO, METTL3, METTL14, and WTAP (Figure 4C–F). Furthermore, both the biotinylated probe of circSTAG1 and the RNA pull-down assay showed that circSTAG1 probe could pull down a higher level of ALKBH5 than the circControl probe (Figure S12A). CatRAPID algorithm was used to predict the binding region of circSTAG1 and RNA demethylase ALKBH5. As shown in Figure 4G, the amino acid sequence (345–395) of ALKBH5 revealed a high score. To validate the association of

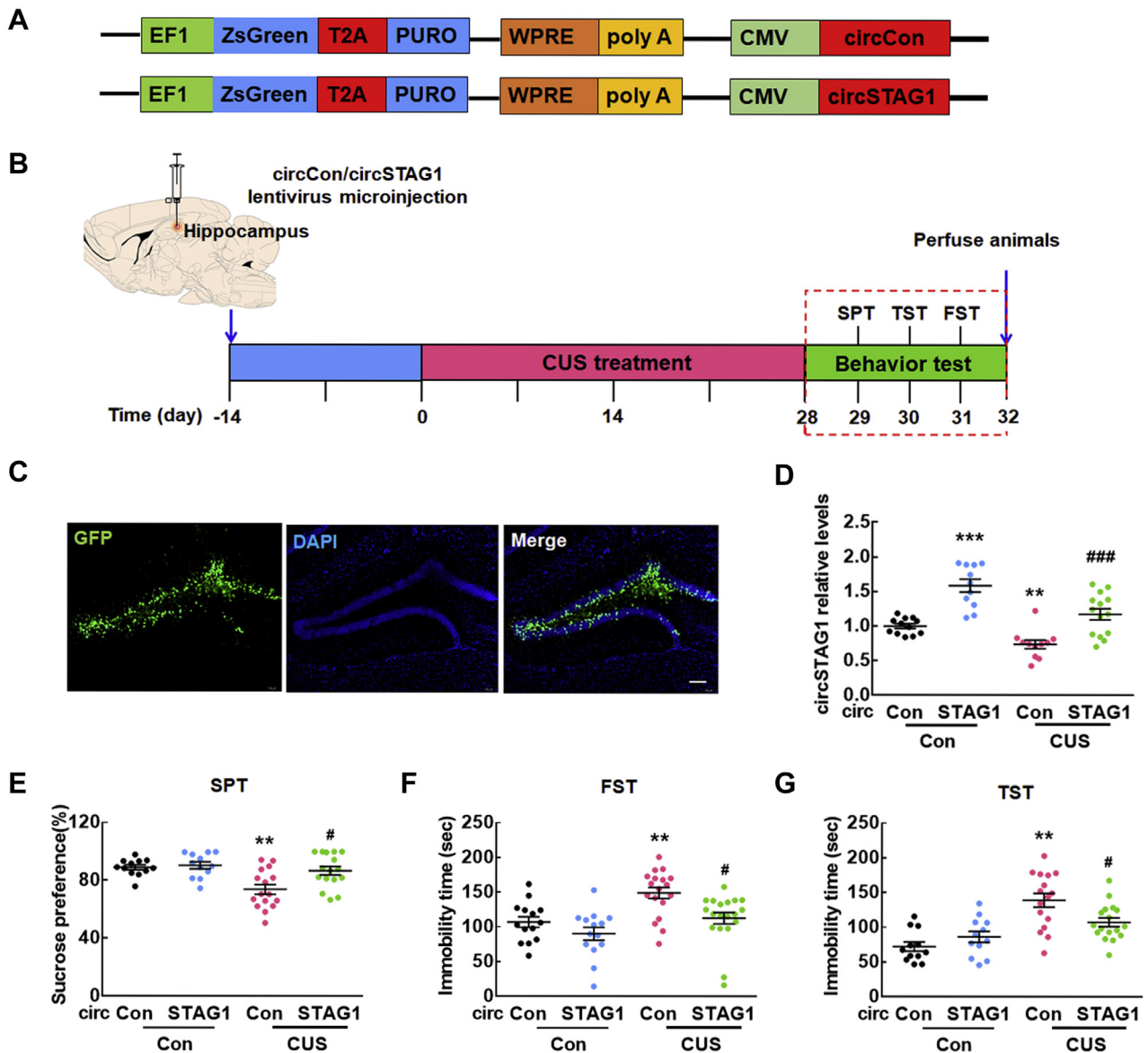


Figure 2. Overexpression of circSTAG1 ameliorated depressive-like behaviors. **(A)** Schematic of the lentivirus vector encoding circSTAG1. **(B)** Experimental procedure and timeline. **(C)** Representative images of the mouse hippocampus microinjected with GFP lentiviruses. Mice were sacrificed 2 weeks after microinjection, and GFP expression was measured. Scale bar = 100 μ m. **(D)** circSTAG1 levels were measured after microinjection with/without CUS treatment. $n = 6$ – 10 /each group. circSTAG1: $F_{1,44} = 61.18$, $p < .001$; CUS: $F_{1,44} = 21.95$, $p < .001$; interaction: $F_{1,44} = 5.151$, $p = .0381$. **(E–G)** Effects of circSTAG1 lentivirus microinjection on the depressive-like behaviors in CUS mice. SPT **(E)**, FST **(F)**, and TST **(G)** were measured after 4 weeks of CUS exposure. $n = 13$ – 16 /each group. SPT–circSTAG1: $F_{1,52} = 6.435$, $p = .0142$; CUS: $F_{1,52} = 10.870$, $p = .0018$; interaction: $F_{1,52} = 4.091$, $p = .0402$; TST–circSTAG1: $F_{1,52} = 7.046$, $p = .0179$; CUS: $F_{1,52} = 7.966$, $p = .0011$; interaction: $F_{1,52} = 4.866$, $p = .019$; FST–circSTAG1: $F_{1,52} = 7.046$, $p = .0109$; CUS: $F_{1,52} = 7.966$, $p = .0071$; interaction: $F_{1,52} = 7.358$, $p = .0486$. All data are presented as mean \pm SEM. $**p < .01$ and $***p < .001$ vs. the circControl group without CUS treatment; $\#p < .05$ and $###p < .001$ vs. the circControl group with CUS treatment. circ, circular RNA; CMV, cytomegalovirus; Con, control; CUS, chronic unpredictable stress; EF1, elongation factor 1; FST, forced swim test; GFP, green fluorescent protein; PURO, puromycin; SPT, sucrose preference test; TST, tail suspension test.

circSTAG1 and ALKBH5, we generated the 3Flag-labeled ALKBH5 lacking amino acid sequence 345–395 (Figure 4H). The deficient ALKBH5 hardly absorbed circSTAG1 (Figure 4I). The binding sequence of circSTAG1 with ALKBH5 was predicated by the catRAPID algorithm (Figure S12B). We further constructed circSTAG1 mutation plasmid, which mutated the binding sequence of circSTAG1 with ALKBH5.

Comparing with the circSTAG1 mutation group, circSTAG1 overexpression in astrocytes showed higher binding with ALKBH5 (Figure S12C).

Redistribution of ALKBH5 After CUS Treatment

Having determined that overexpression or knockdown of circSTAG1 did not affect the expression of ALKBH5 protein in

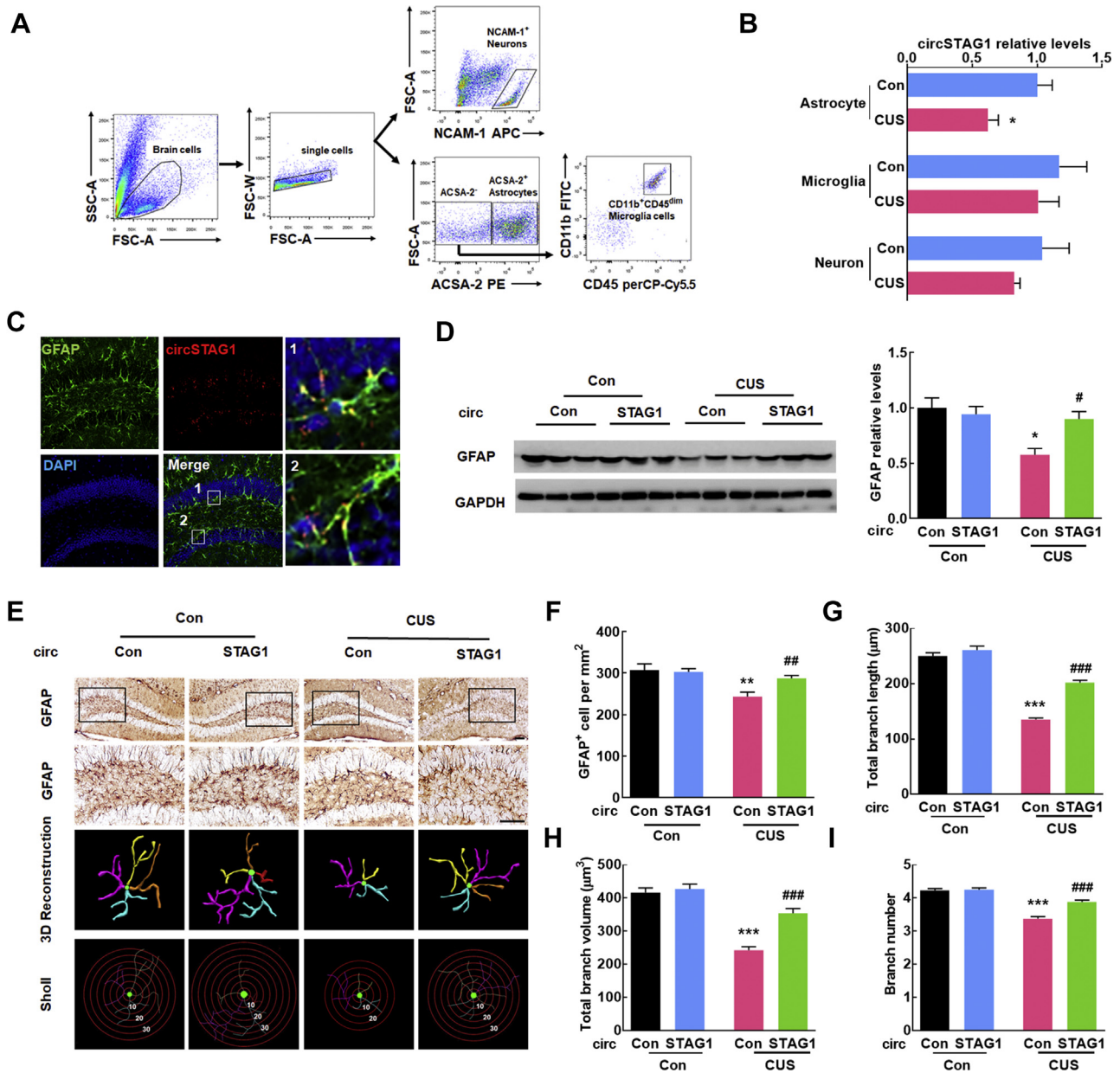


Figure 3. Effect of circSTAG1 on astrocyte loss in the CUS mouse hippocampus. **(A)** Schematic of neuron, astrocyte, and microglia cell isolation in the mouse brain. **(B)** Total RNA extracted from neurons, astrocytes, and microglia cells was separated by flow cytometric cell sorting, and circSTAG1 levels were measured by real-time polymerase chain reaction. $n = 6-8$ /each group. $t_5 = 2.813$, $*p < .05$ vs. the Con group. **(C)** Colocalization of GFAP and circSTAG1 in the mouse hippocampus. Numbered rectangular areas were respectively enlarged. Scale bar = 200 μm . **(D)** Representative Western blots of the GFAP expression after circSTAG1 lentivirus microinjection with/without CUS treatment. $n = 6-8$ /each group. circSTAG1: $F_{1,8} = 7.175$, $p = .028$; CUS: $F_{1,8} = 14.37$, $p = .0053$; interaction: $F_{1,8} = 6.907$, $p = .0303$. **(E)** Effect of circSTAG1 on astrocyte dysfunction induced by CUS. Representative images of astrocyte immunostaining for GFAP in the mouse hippocampus, followed by 3D reconstruction and Sholl analysis. Scale bar = 50 μm . **(F)** Quantification of GFAP-positive cells per mm^2 in the mouse hippocampus. $n = 4-6$ mice/group. circSTAG1: $F_{1,18} = 4.758$, $p = .0427$; CUS: $F_{1,18} = 13.18$, $p = .0019$; interaction: $F_{1,18} = 6.803$, $p = .0178$. **(G-I)** Quantification of average branch length **(G)**, total branch volume **(H)**, and total branch number **(I)**. $n = 4-6$ mice/group, 40 cells/group. Average branch length—circSTAG1: $F_{1,236} = 53.59$, $p < .001$; CUS: $F_{1,236} = 269.40$, $p < .001$; interaction: $F_{1,236} = 28.24$, $p < .001$; branch volume—circSTAG1: $F_{1,236} = 20.55$, $p < .001$; CUS: $F_{1,236} = 82.67$, $p < .001$; interaction: $F_{1,236} = 13.59$, $p < .001$; branch number—circSTAG1: $F_{1,236} = 18.77$, $p < .001$; CUS: $F_{1,236} = 104.10$, $p < .001$; interaction: $F_{1,236} = 16.42$, $p < .001$. $*p < .05$, $**p < .01$, and $***p < .001$ vs. the circControl group without CUS treatment; # $p < .05$, ## $p < .01$, and ### $p < .001$ vs. the circControl group with CUS treatment. ACSA-2 PE, astrocyte cell surface antigen-2 phycoerythrin; circ, circular RNA; Con, control; CUS, chronic unpredictable stress; FSC-A, forward scatter area; NCAM-1 APC, neural adhesion molecule-1 allophycocyanin; SSC-A, side scatter area.

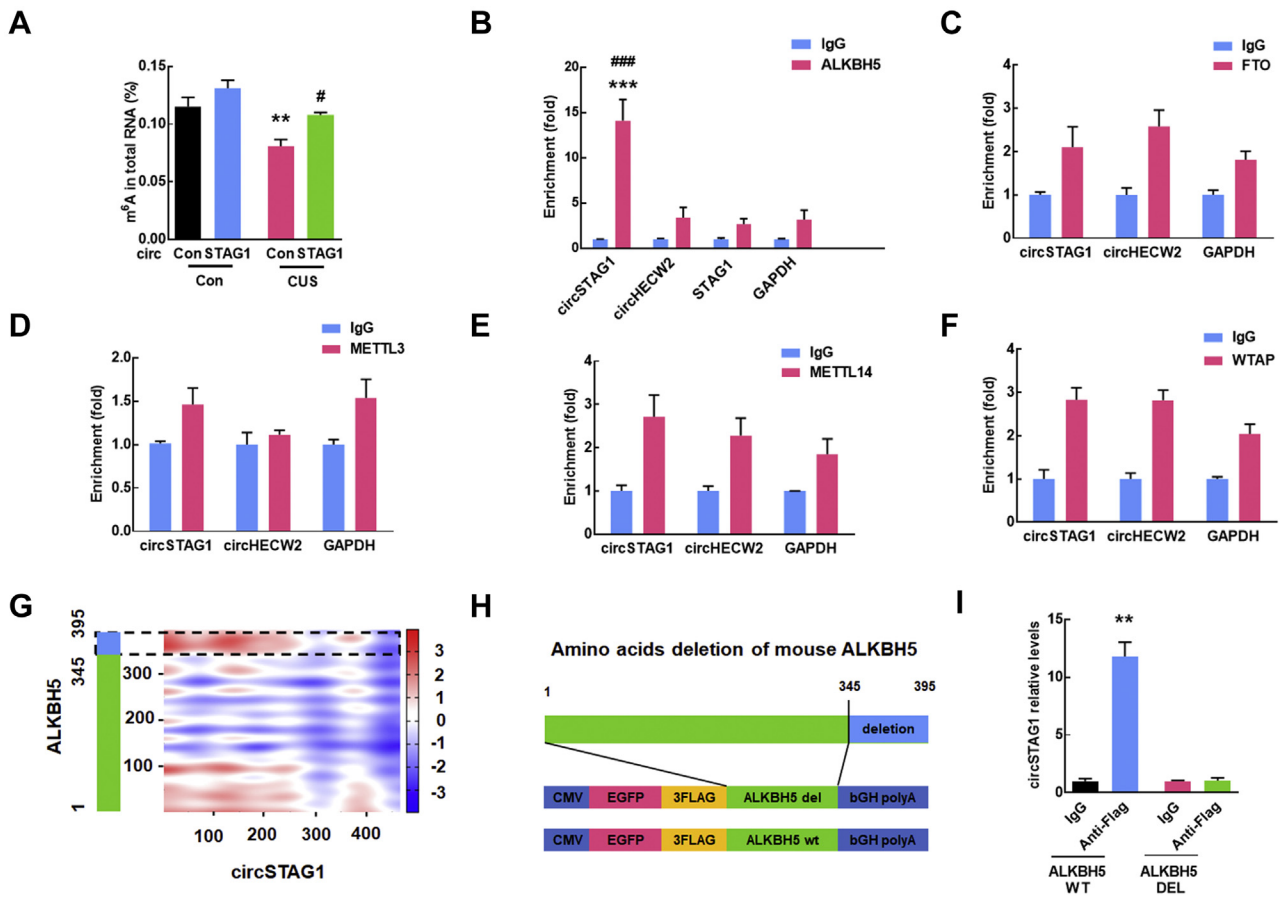


Figure 4. circSTAG1 bound with ALKBH5. **(A)** Total RNA was extracted from the mouse hippocampus, and m⁶A levels were determined as a percentage of all adenosine residues in RNA. *n* = 7–10/each group. circSTAG1: $F_{1,31} = 16.11, p < .001$; CUS: $F_{1,31} = 26.87, p < .001$; interaction: $F_{1,31} = 7.648, p = .0268$. ***p* < .01 vs. the circControl group without CUS treatment; #*p* < .05 vs. the circControl group with CUS treatment. **(B)** Interaction between circSTAG1 and ALKBH5 was validated by RNA immunoprecipitation in the mouse hippocampus. Data are presented as mean ± SEM of 3 independent experiments. Each experiment was undertaken in a pooled sample of two mouse hippocampi. $F_{7,16} = 19.44$. ****p* < .001 vs. ALKBH5 pull-down of circHECW2; ###*p* < .001 vs. ALKBH5 pull-down of GAPDH mRNA. **(C–F)** Interaction between circSTAG1 and FTO **(C)**, METTL3 **(D)**, METTL14 **(E)**, and WTAP **(F)** was validated by RNA immunoprecipitation in the mouse hippocampus. FTO: $F_{5,12} = 6.319, p = .8064$ vs. FTO pull-down of circHECW2, $p = .9701$ vs. FTO pull-down of GAPDH mRNA. METTL3: $p = .4811$ vs. METTL3 pull-down of circHECW2, $p = .9983$ vs. METTL3 pull-down of GAPDH mRNA. METTL14: $F_{5,12} = 5.973, p = .9149$ vs. METTL14 pull-down of circHECW2, $p = .4022$ vs. METTL14 pull-down of GAPDH mRNA. WTAP: $F_{5,12} = 19.93, p > .9999$ vs. WTAP pull-down of circHECW2, $p = .1322$ vs. WTAP pull-down of GAPDH mRNA. **(G)** The catRAPID algorithm was applied to predict the interaction between circSTAG1 and ALKBH5. **(H)** Schematic for deficient ALKBH5. **(I)** The interaction between circSTAG1 and ALKBH5 was validated by RNA immunoprecipitation in astrocytes with WT ALKBH5 and DEL ALKBH5. Anti-Flag: $F_{1,8} = 72.19, p < .001$; ALKBH5 DEL: $F_{1,8} = 73.68, p < .001$; interaction: $F_{1,8} = 72.19, p < .001$. ***p* < .01 vs. ALKBH5 WT-IgG group. bGH, bovine growth hormone; circ, circular RNA; CMV, cytomegalovirus; Con, control; CUS, chronic unpredictable stress; DEL, deletion; EGFP, enhanced green fluorescent protein; m⁶A, N⁶-methyladenosine; WT, wild-type.

astrocyte, we next sought to examine the ALKBH5 expression in CUS mice. There is no significant difference in the expression of ALKBH5 protein in the hippocampus of CUS mice compared with that of control group (Figure 5A). However, ALKBH5 expression was notably decreased in the cytoplasm and increased in the nucleus after CUS treatment (Figure 5B, C). Given these, we believe that in CUS mice ALKBH5 redistributed from the cytoplasm to the nucleus. This finding was confirmed in vitro given that overexpression of circSTAG1 increased ALKBH5 in the astrocyte cytoplasm and decreased ALKBH5 in the nucleus (Figure 5D, E). Full-length images are shown in Figure S13. This finding was

further confirmed by immunofluorescence staining (Figure 5F). We next sought to investigate the role of ALKBH5 in the depressive-like behavior of CUS mice by microinjecting either the Control-GFP or the shRNA-GFP lentivirus into the mouse hippocampus (Figure 5G). For depressive-like behaviors, CUS treatment decreased sucrose preference compared with the control group; the deficit was notably rescued by ALKBH5 shRNA (Figure 5H). Moreover, microinjection of ALKBH5 shRNA significantly inhibited the increase of immobility induced by CUS as shown in Figure 5I (forced swim test) and Figure 5J (tail suspension test).

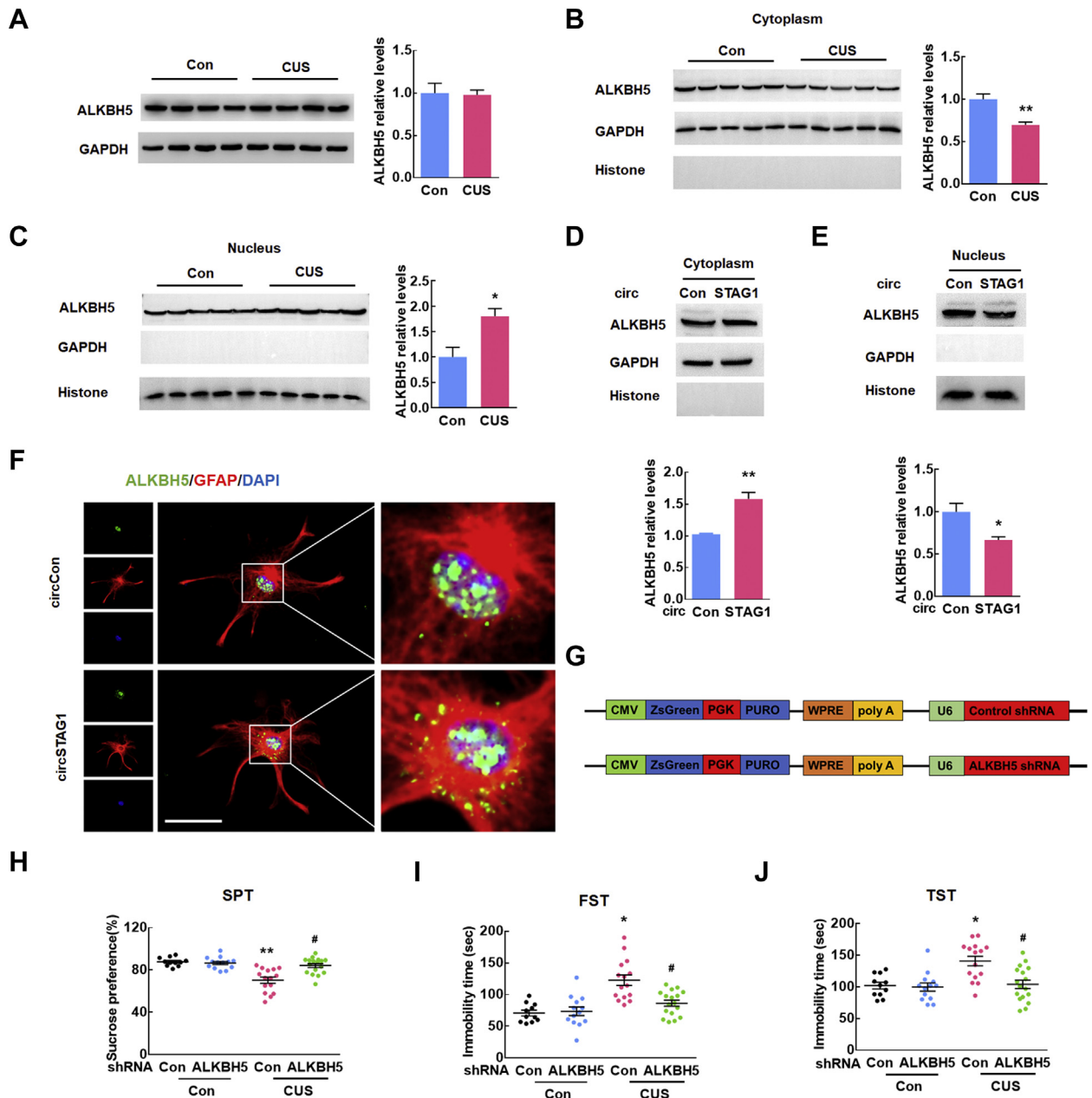


Figure 5. CUS treatment altered the subcellular localization of ALKBH5. **(A)** Representative Western blots of ALKBH5 expression in the mouse hippocampus after 4 weeks of CUS. $n = 8$ /each group. **(B, C)** ALKBH5 expression in the mouse hippocampus cytoplasm **(B)** and nucleus **(C)** after 4 weeks of CUS. $n = 10$ /each group. Data are presented as mean \pm SEM. Cytoplasm: $t_8 = 4.418$; nucleus: $t_8 = 3.346$; * $p < .05$ and ** $p < .01$ vs. the control group. **(D, E)** Representative Western blots of ALKBH5 expression in the cytoplasm **(D)** and nucleus **(E)** of astrocytes transfected with circSTAG1 plasmid. All data are presented as mean \pm SEM. Cytoplasm: $t_4 = 5.557$; nucleus: $t_4 = 3.047$; * $p < .05$ and ** $p < .01$ vs. the circControl group using Student's t test. **(F)** Astrocytes were subjected to immunocytochemistry analysis of GFAP and ALKBH5 protein after circSTAG1 plasmid transfection. Scale bar = 50 μ m. **(G)** Schematic of the lentivirus vector encoding ALKBH5 shRNA. Construction of ALKBH5 shRNA was based on the ALKBH5 siRNA. **(H–J)** Effects of circSTAG1 lentivirus microinjection on the depressive-like behaviors in CUS mice. SPT **(H)**, FST **(I)**, and TST **(J)** were measured after 4 weeks of CUS exposure. $n = 11$ –17/each group. All data are presented as mean \pm SEM. SPT—ALKBH5 shRNA: $F_{1,52} = 8.898$, $p = .0043$; CUS: $F_{1,52} = 21.52$, $p < .001$; interaction: $F_{1,52} = 12.30$, $p < .001$; FST—ALKBH5 shRNA: $F_{1,52} = 6.636$, $p = .0129$; CUS: $F_{1,52} = 24.31$, $p < .001$; interaction: $F_{1,52} = 8.907$, $p = 0.0043$; TST—ALKBH5 shRNA: $F_{1,52} = 7.856$, $p = .0071$; CUS: $F_{1,52} = 9.803$, $p = .0029$; interaction: $F_{1,52} = 6.280$, $p = .0154$. * $p < .05$ and ** $p < .01$ vs. the shRNA control group without CUS treatment; # $p < .05$ vs. the shRNA control group with CUS treatment. circ, circular RNA; CMV, cytomegalovirus; Con, control; CUS, chronic unpredictable stress; FST, forced swim test; PGK, phosphoglycerate kinase; PURO, puromycin; shRNA, short hairpin RNA; siRNA, small interfering RNA; SPT, sucrose preference test; TST, tail suspension test.

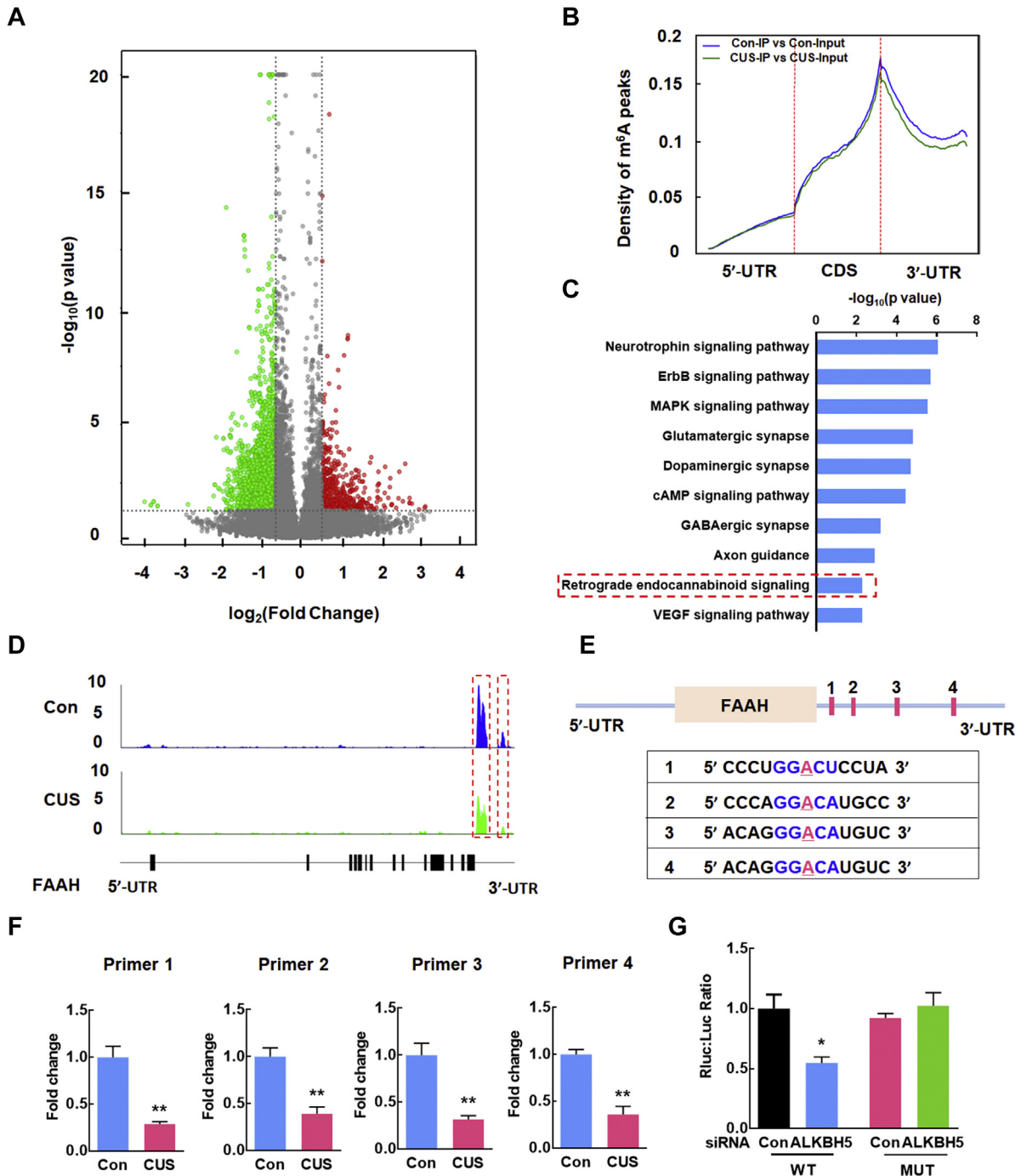


Figure 6. ALKBH5 regulated m⁶A modification of FAAH mRNA in the CUS mouse hippocampus. **(A)** Significant upregulation and downregulation in m⁶A methylation of mRNA (fold change ≥ 1.5). Total RNA was extracted from 5 control and 5 CUS mouse hippocampi, and MeRIP sequence analysis was performed after mRNA purification. **(B)** Distribution of m⁶A peaks across the 5'-UTR, CDS, and 3'-UTR of mRNA in the control and CUS mouse hippocampus. **(C)** The top 10 significantly enriched depression-associated pathways with downregulated m⁶A peak transcripts. **(D)** Abundant m⁶A in FAAH mRNA transcripts. M⁶A peaks in red rectangles have significantly reduced abundance (fold change ≥ 1.5). **(E)** Predictive m⁶A sites in the 3'-UTR of FAAH mRNA. **(F)** Specific primers against m⁶A sites were designed to amplify products. $n = 3$ /each group. Primer 1: $t_4 = 5.942$; primer 2: $t_4 = 5.192$; primer 3: $t_4 = 5.142$; primer 4: $t_4 = 6.372$. ** $p < .01$ vs. the control group. **(G)** Luciferase assays were performed in astrocytes transfected with WT or mutant luciferase FAAH 3'-UTR reporters. ALKBH5 siRNA: $F_{1,8} = 17.80$, $p = .0029$; MUT: $F_{1,8} = 12.47$, $p = .0077$; interaction: $F_{1,8} = 19.69$, $p = .0022$. * $p < .05$ vs. the siRNA control group with WT plasmid treatment. cAMP, cyclic adenosine monophosphate; Con, control; CUS, chronic unpredictable stress; GABA, gamma-aminobutyric acid; IP, immunoprecipitation; M⁶A, N⁶-methyladenosine; MAPK, mitogen-activated protein kinase; MeRIP, methylated RNA immunoprecipitation; mRNA, messenger RNA; MUT, mutant; siRNA, small interfering RNA; UTR, untranslated region; VEGF, vascular endothelial growth factor; WT, wild-type.

ALKBH5 Regulates m⁶A Modification of FAAH mRNA in the CUS Mouse Hippocampus

To explore the downstream molecule potentially involved in MDD, we performed a transcriptome-wide detection of m⁶A modification in CUS mouse hippocampus samples. A volcano plot showed that m⁶A modification of 713 peak regions in transcripts increased and 2939 peak regions in transcripts decreased after CUS treatment (Figure 6A). Reduction of m⁶A modification occurred mainly in the 3'-UTR, not the 5'-UTR or coding region (Figure 6B). Because m⁶A modification was decreased in the CUS hippocampus, we mainly investigated the decreased 2939 peak regions. To further explore the target transcript involved in regulation of depression, we analyzed these transcripts with decreased m⁶A modification by the Kyoto Encyclopedia of Genes and Genomes. The top 10 pathways associated with depression are listed in Figure 6C. In the top 10 pathways, 245 peak regions of transcripts have been ranked by fold change, and the top 10 m⁶A decreased peak regions are listed in Table S6. FAAH, a mood-associated gene modulating depression and anxiety, transcript ranked the first (28,29). Further analysis showed that m⁶A modification was decreased in two peak regions (chr4:115996668-115996878 and chr4:115997804-115998403) in the 3'-UTR of FAAH (Figure 6D). Sequence analysis via SRAMP, a sequence-based m⁶A modification site predictor, revealed 4 positions matching the 5'-RRACH-3' m⁶A consensus sequence in the two peak regions of FAAH (Figure 6E). The m⁶A status of each site was further measured by methylated RNA immunoprecipitation of fragmented RNA. We designed 4 pairs of primers against the m⁶A sites to amplify products about 100 bp, and significant difference was found at each m⁶A site (Figure 6F). Luciferase assays were performed comparing wild-type and mutant m⁶A sites with and without ALKBH5 siRNA treatment, suggesting that the mutation prevented methylation and increased the stability of FAAH mRNA (Figure 6G).

circSTAG1 Regulates m⁶A Methylation of FAAH mRNA via ALKBH5

Knowing that m⁶A methylation of FAAH mRNA was decreased in the CUS mouse hippocampus, we next sought to further examine the expression and function of FAAH. As shown in Figure 7A, both FAAH mRNA and FAAH were significantly increased in the mouse hippocampus after CUS treatment, which was consistent with the decreased m⁶A modification in the 3'-UTR of FAAH mRNA. ALKBH5 siRNA treatment reduced ALKBH5, FAAH, and FAAH mRNA expression (Figure 7B, C). Overexpression of circSTAG1 in astrocytes also reduced FAAH and FAAH mRNA expression (Figure 7D). Cotransfection of ALKBH5 siRNA and circSTAG1 siRNA showed that circSTAG1 siRNA increased the expression of FAAH, which was significantly inhibited by ALKBH5 siRNA (Figure 7E). These findings suggest that circSTAG1 affected the stability of FAAH mRNA via ALKBH5.

We next examined the effect of circSTAG1 on astrocyte survival *in vitro*. Corticosterone was used to mimic the depression context. As shown in Figure S14A, treatment of astrocytes with 9 μ M corticosterone for 72 hours reduced the number of astrocytes. Pretreatment of astrocytes with

exogenous circSTAG1 inhibited the decreased cell viability induced by corticosterone (Figure 7F), which was rescued by circSTAG1 siRNA (Figure S14B). Knockdown of the expression of ALKBH5 or FAAH also significantly inhibited the decreased cell viability induced by corticosterone (Figure 7F). Moreover, the effect of circSTAG1 siRNA on further decreased astrocyte viability was attenuated by ALKBH5 siRNA, suggesting a functional connection between circSTAG1 and ALKBH5 (Figure 7G).

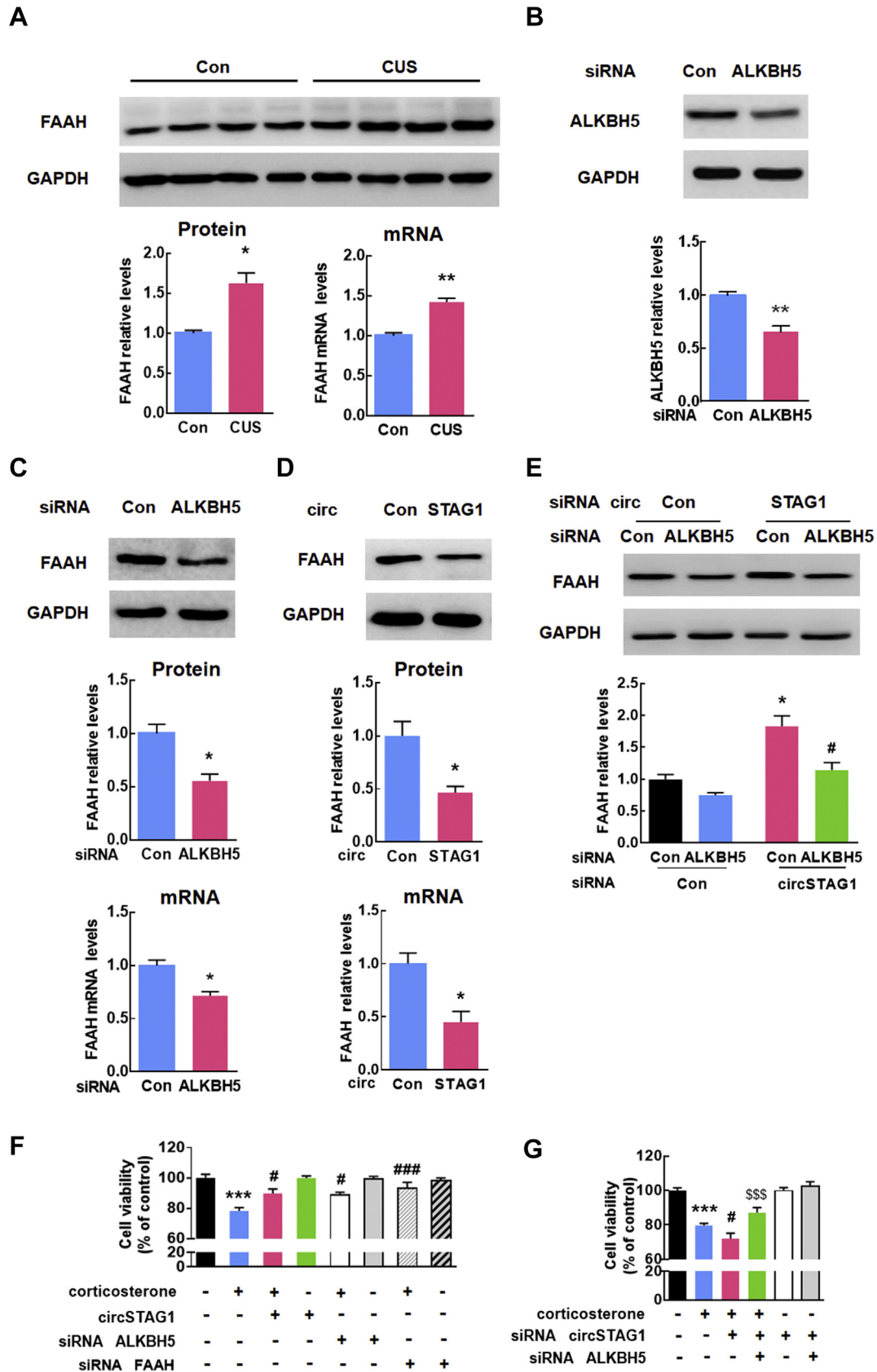
DISCUSSION

Our study demonstrated that circSTAG1 is downregulated in the peripheral blood of both patients with MDD and CUS mouse models. Decreased expression of circSTAG1 released demethylase ALKBH5, which decreased methylation of FAAH, affecting the stability of FAAH mRNA as well as its expression with subsequent astrocyte dysfunction (Figure S15). Upregulation of circSTAG1 may thus represent a potential therapeutic target for depression. This study sheds light on the functional link between circSTAG1 and m⁶A methylation and provides a new idea about the development of preventive strategy and effective treatment for MDD.

Our previous study demonstrated that circDYM is a potential therapeutic target for MDD, which led us to further dissect other circRNAs involved in MDD using high-throughput sequencing. CircRNA-mm9_circ_0015149, known as circSTAG1, was downregulated in CUS mice (GEO accession number: GSE135343). This finding was confirmed in patients with MDD. Moreover, levels of circSTAG1 in peripheral blood of patients with MDD were negatively correlated with HAMD-17 items, HAMD-24 items, and Ruminative Responses Scale-Brooding scores, which are important evaluation indices of MDD. Together, our results indicate that dysregulation of circSTAG1 in peripheral blood is related to the pathophysiology of MDD.

To our knowledge, this is the first study to demonstrate the functional link between circSTAG1 and m⁶A methylation in the context of MDD. M⁶A, particularly in the 3'-UTR near the translation termination codon, is the most common modification of mRNA in higher eukaryotic cells (30). M⁶A is a reversible modification in mRNA and participates in regulation of mRNA processing, translation, and stability. RNA m⁶A methylation is mediated by methylases and demethylases. The hippocampus of CUS mice showed a significant decrease in m⁶A of total RNA, suggesting nucleus methylase downregulation or demethylase upregulation. A previous study also indicated that global m⁶A was regulated in total RNA in a region-dependent manner, with the RNA m⁶A level increased in the amygdala and decreased in the prefrontal cortex in mice injected with corticosterone (17). These findings suggest that dysregulation of the RNA m⁶A methylation response may be responsible for stress-related psychiatric disorders.

Given the decrease of circSTAG1 in CUS mice, we hypothesize that certain demethylases, which interact with circSTAG1 in the cytoplasm, were freed and moved into the nucleus, resulting in the downregulation of m⁶A. One potential demethylase is ALKBH5, which in one clinical trial was shown to confer MDD risk in the Chinese population (19). ALKBH5 is a



dioxygenase that uses ketoglutarate and O₂ as substrates in the m⁶A demethylation process. In the study reported here, we tested the hypothesis that overexpression of circSTAG1 captured ALKBH5 and decreased its translocation into the nucleus, leading to increased m⁶A methylation of FAAH mRNA and degradation of FAAH with subsequent attenuation of astrocyte dysfunction.

Increasing evidence indicates that m⁶A methylation affects mRNA stability and regulates pathological and physiological processes (31). In our study, m⁶A modulation was shown to regulate the stability of FAAH mRNA. FAAH, which is an integral membrane enzyme, degrades the fatty acid amide family, including the endocannabinoid anandamide. The effect of the endocannabinoid system on depression has been established in previous studies (32,33). FAAH knockdown and inhibitors lead to antidepressant phenotypes in rodents without the serious side effects observed with direct cannabinoid receptor agonists (34,35). In our study, circSTAG1 overexpression induced FAAH deficiency and, consistent with previous studies, ameliorated depressive-like behaviors. The down-regulation of FAAH by circSTAG1 may also restore astrocyte loss to improve depressive-like behaviors.

In the current study, circSTAG1 may bind with demethylase ALKBH5 to regulate its target FAAH mRNA methylation and thereby ameliorate depressive-like behaviors. These findings are consistent with previous studies where it was found that circFoxo3 is involved in cell cycle progression by generating a ternary complex with p21 and CDK2 (36). Moreover, circYAP, which is mainly expressed in the cytoplasm, significantly decreased Yap protein and suppressed cell proliferation, migration, and colony formation via PABP binding (37). In addition to binding with enzymes/proteins, circRNAs exert their biological functions via other mechanisms. Accumulating evidence indicates that circRNA HRCR (heart-related circRNA) binds miR-223 to regulate cardiac hypertrophy and heart failure (38), and another circRNA, SRY (sex-determining region Y), acts as a sponge for miR-138 (13). In addition, some circRNAs have demonstrated excess ability to encode proteins or peptides (39). Given these complexities, although we demonstrated that m⁶A methylation of FAAH lies downstream of circSTAG1, we could not rule out the possibility that other mechanisms may underlie the functions of circSTAG1.

Taken together, findings of this study revealed the functional link between circSTAG1 and ALKBH5 for the first time; circSTAG1 captured ALKBH5 and decreased its translocation

into the nucleus, leading to increased m⁶A methylation of FAAH mRNA and degradation of FAAH in astrocytes, with subsequent attenuation of depressive-like behaviors. Our study provides proof-of-concept evidence that restoration of circSTAG1 attenuated depressive-like behaviors through the regulation of astrocyte function. Thus, circSTAG1 may be a promising target for therapeutic intervention in MDD.

ACKNOWLEDGMENTS AND DISCLOSURES

This work was funded by the National Natural Science Foundation of China (Grant Nos. 81673410 [to HY], 81973304 [to YZ], and 81903591 [to YB]), the National Key Research and Development Program of China (Grant No. 2017YFA0104303 [to HY]), the International Cooperation and Exchange of the National Natural Science Foundation of China (Grant No. 81761138048 [to HY]), the Jiangsu Innovation and Entrepreneurship Team Program (to HY), the Natural Science Foundation of Jiangsu Province (Grant No. BK20191265 [to YZ]), the Fundamental Research Funds for the Central Universities (Grant Nos. 2242019K40133 [to YB] and 2242020K40134 [to BH]), National Science and Technology Major Project (Grant No. 2020ZX09201015 [to HY]), and the Postgraduate Research and Practice Innovation Program of Jiangsu Province (Grant No. KYCX18_0166 [to RH]).

HY planned and designed the research and wrote the manuscript. RH performed the CUS, behavior test, immunostaining, and Western blot. YZ performed the immunostaining. YB performed the flow cytometry sorting. BH designed the primers. MJ performed the 3D reconstruction. BC performed the lentivirus microinjection. LY performed the fluorescence in situ hybridization. YW performed the real-time PCR. HoZ and HaZ recruited patients with MDD and collected clinical patient blood samples. CX and ZZ performed the analysis of clinical samples.

The authors report no biomedical financial interests or potential conflicts of interest.

ARTICLE INFORMATION

From the Department of Pharmacology (RH, YZ, YB, BH, MJ, BC, LY, YW, HY), School of Medicine, Southeast University; Department of Neurology (CX, ZZ), Affiliated ZhongDa Hospital, Institute of Neuropsychiatry, Southeast University; and Institute of Life Sciences (HY), Key Laboratory of Developmental Genes and Human Disease, Southeast University, Nanjing; and Co-innovation Center of Neuroregeneration (HY), Nantong University, Nantong, Jiangsu; and Department of Psychology (HoZ, ZZ) and Second Affiliated Hospital (HoZ, HaZ, ZZ), Xinxiang Medical University, Xinxiang, Henan, China.

Address correspondence to Honghong Yao, Ph.D., Department of Pharmacology, Medical School of Southeast University, Nanjing 210009, Jiangsu, China; E-mail: yaohh@seu.edu.cn.

Received Aug 15, 2019; revised Feb 14, 2020; accepted Feb 18, 2020.

Supplementary material cited in this article is available online at <https://doi.org/10.1016/j.biopsych.2020.02.018>.

Figure 7. circSTAG1 regulated N⁶-methyladenosine of FAAH mRNA via ALKBH5. **(A)** Representative Western blots of FAAH expression in the mouse hippocampus after 4 weeks of CUS. $t_{14} = 4.770$. FAAH mRNA expression was measured by real-time polymerase chain reaction. $t_{14} = 7.096$. $n = 8$ /each group. $^*p < .05$ and $^{**}p < .01$ vs. the control group. **(B)** Representative Western blots of ALKBH5 expression in astrocytes with/without ALKBH5 siRNA transfection. $t_4 = 5.567$. $^{**}p < .01$ vs. the control group. **(C)** Effect of ALKBH5 siRNA on the expression of FAAH and FAAH mRNA. Protein: $t_4 = 4.192$; mRNA: $t_4 = 4.537$. $^*p < .05$ vs. the control group. **(D)** Effect of circSTAG1 on the expression of FAAH and FAAH mRNA. Protein: $t_4 = 3.623$; mRNA: $t_4 = 3.870$. $^*p < .05$ vs. the control group. **(E)** Effect of circSTAG1 and ALKBH5 siRNA on the expression of FAAH. ALKBH5 siRNA: $F_{1,8} = 20.97$, $p = .0018$; circSTAG1 siRNA: $F_{1,8} = 35.76$, $p = .0083$; interaction: $F_{1,8} = 4.557$, $p = .0353$. $^*p < .05$ vs. the siRNA control group; $^{\#}p < .05$ vs. the siRNA control group with siRNA circSTAG1 treatment. **(F)** Protective effect of circSTAG1, ALKBH5 siRNA, and FAAH siRNA on astrocyte loss induced by corticosterone. $F_{7,72} = 10.45$. $^{***}p < .001$ vs. the control group; $^{\#}p < .05$ and $^{###}p < .001$ vs. the corticosterone group. **(G)** Effect of circSTAG1 siRNA and ALKBH5 siRNA on astrocyte loss induced by corticosterone. $F_{5,30} = 29.57$. $^{***}p < .001$ vs. the control group; $^{\#}p < .05$ vs. the corticosterone group; $^{SSS}p < .001$ vs. the corticosterone group with circSTAG1 siRNA treatment. circ, circular RNA; Con, control; CUS, chronic unpredictable stress; mRNA, messenger RNA; siRNA, small interfering RNA.

REFERENCES

- Collins PY, Patel V, Joestl SS, March D, Insel TR, Daar AS, *et al.* (2011): Grand challenges in global mental health. *Nature* 475:27–30.
- Whiteford HA, Degenhardt L, Rehm J, Baxter AJ, Ferrari AJ, Erskine HE, *et al.* (2013): Global burden of disease attributable to mental and substance use disorders: Findings from the Global Burden of Disease Study 2010. *Lancet* 382:1575–1586.
- Global Burden of Disease Study Collaborators (2015): Global, regional, and national incidence, prevalence, and years lived with disability for 301 acute and chronic diseases and injuries in 188 countries, 1990–2013: A systematic analysis for the Global Burden of Disease Study 2013. *Lancet* 386:743–800.
- Bromet E, Andrade LH, Hwang I, Sampson NA, Alonso J, de Girolamo G, *et al.* (2011): Cross-national epidemiology of DSM-IV major depressive episode. *BMC Med* 9:90.
- Chen YW, Dilsaver SC (1996): Lifetime rates of suicide attempts among subjects with bipolar and unipolar disorders relative to subjects with other Axis I disorders. *Biol Psychiatry* 39:896–899.
- Pena CJ, Bagot RC, Labonte B, Nestler EJ (2014): Epigenetic signaling in psychiatric disorders. *J Mol Biol* 426:3389–3412.
- Cui X, Niu W, Kong L, He M, Jiang K, Chen S, *et al.* (2016): hsa_circRNA_103636: Potential novel diagnostic and therapeutic biomarker in major depressive disorder. *Biomark Med* 10:943–952.
- Papakostas GI, Ionescu DF (2015): Towards new mechanisms: An update on therapeutics for treatment-resistant major depressive disorder. *Mol Psychiatry* 20:1142–1150.
- Yuan H, Mischoulon D, Fava M, Otto MW (2018): Circulating microRNAs as biomarkers for depression: Many candidates, few finalists. *J Affect Disord* 233:68–78.
- Murrough JW, Abdallah CG, Mathew SJ (2017): Targeting glutamate signalling in depression: Progress and prospects. *Nat Rev Drug Discov* 16:472–486.
- Mrazek DA, Hornberger JC, Altar CA, Degtjar I (2014): A review of the clinical, economic, and societal burden of treatment-resistant depression: 1996–2013. *Psychiatr Serv* 65:977–987.
- Memczak S, Jens M, Elefsinioti A, Torti F, Krueger J, Rybak A, *et al.* (2013): Circular RNAs are a large class of animal RNAs with regulatory potency. *Nature* 495:333–338.
- Hansen TB, Jensen TI, Clausen BH, Bramsen JB, Finsen B, Damgaard CK, *et al.* (2013): Natural RNA circles function as efficient microRNA sponges. *Nature* 495:384–388.
- Han B, Zhang Y, Zhang Y, Bai Y, Chen X, Huang R, *et al.* (2018): Novel insight into circular RNA HECTD1 in astrocyte activation via autophagy by targeting MIR142-TIPARP: Implications for cerebral ischemic stroke. *Autophagy* 14:1164–1184.
- Zhang Y, Du L, Bai Y, Han B, He C, Gong L, *et al.* (2020): CircDYM ameliorates depressive-like behavior by targeting miR-9 to regulate microglial activation via HSP90 ubiquitination. *Mol Psychiatry* 25:1175–1190.
- Zheng Q, Bao C, Guo W, Li S, Chen J, Chen B, *et al.* (2016): Circular RNA profiling reveals an abundant circHIPK3 that regulates cell growth by sponging multiple miRNAs. *Nat Commun* 7:11215.
- Engel M, Eggert C, Kaplick PM, Eder M, Roh S, Tietze L, *et al.* (2018): The role of m⁶A-m-RNA methylation in stress response regulation. *Neuron* 99:389–403.e9.
- Samaan Z, Anand SS, Zhang X, Desai D, Rivera M, Pare G, *et al.* (2013): The protective effect of the obesity-associated rs9939609 A variant in fat mass- and obesity-associated gene on depression. *Mol Psychiatry* 18:1281–1286.
- Du T, Rao S, Wu L, Ye N, Liu Z, Hu H, *et al.* (2015): An association study of the m6A genes with major depressive disorder in Chinese Han population. *J Affect Disord* 183:279–286.
- Cao X, Li LP, Wang Q, Wu Q, Hu HH, Zhang M, *et al.* (2013): Astrocyte-derived ATP modulates depressive-like behaviors. *Nat Med* 19:773–777.
- Miguel-Hidalgo JJ, Baucom C, Dilley G, Overholser JC, Meltzer HY, Stockmeier CA, *et al.* (2000): Glial fibrillary acidic protein immunoreactivity in the prefrontal cortex distinguishes younger from older adults in major depressive disorder. *Biol Psychiatry* 48:861–873.
- Nagy C, Suderman M, Yang J, Szyf M, Mechawar N, Ernst C, *et al.* (2015): Astrocytic abnormalities and global DNA methylation patterns in depression and suicide. *Mol Psychiatry* 20:320–328.
- Elliott E, Ezra-Nevo G, Regev L, Neufeld-Cohen A, Chen A (2010): Resilience to social stress coincides with functional DNA methylation of the Crf gene in adult mice. *Nat Neurosci* 13:1351–1353.
- Willner P, Muscat R, Papp M (1992): Chronic mild stress-induced anhedonia: A realistic animal model of depression. *Neurosci Biobehav Rev* 16:525–534.
- Barthas F, Humo M, Gilsbach R, Waltisperger E, Karatas M, Leman S, *et al.* (2017): Cingulate overexpression of mitogen-activated protein kinase phosphatase-1 as a key factor for depression. *Biol Psychiatry* 82:370–379.
- Kaufmann FN, Menard C (2018): Inflamed astrocytes: A path to depression led by menin. *Neuron* 100:511–513.
- Leng L, Zhuang K, Liu Z, Huang C, Gao Y, Chen G, *et al.* (2018): Menin deficiency leads to depressive-like behaviors in mice by modulating astrocyte-mediated neuroinflammation. *Neuron* 100:551–563.e7.
- Blankman JL, Cravatt BF (2013): Chemical probes of endocannabinoid metabolism. *Pharmacol Rev* 65:849–871.
- Ogawa S, Kunugi H (2015): Inhibitors of fatty acid amide hydrolase and monoacylglycerol lipase: New targets for future antidepressants. *Curr Neuropharmacol* 13:760–775.
- Wen J, Lv R, Ma H, Shen H, He C, Wang J, *et al.* (2018): Zc3h13 regulates nuclear RNA m⁶A methylation and mouse embryonic stem cell self-renewal. *Mol Cell* 69:1028–1038.e6.
- Geula S, Moshitch-Moshkovitz S, Dominissini D, Mansour AA, Kol N, Salmon-Divon M, *et al.* (2015): Stem cells. m6A mRNA methylation facilitates resolution of naive pluripotency toward differentiation. *Science* 347:1002–1006.
- Huang WJ, Chen WW, Zhang X (2016): Endocannabinoid system: Role in depression, reward and pain control. *Mol Med Rep* 14:2899–2903.
- Meyer JD, Crombie KM, Cook DB, Hillard CJ, Koltyn KF (2019): Serum endocannabinoid and mood changes after exercise in major depressive disorder. *Med Sci Sports Exerc* 51:1909–1917.
- Vinod KY, Xie S, Psychoyos D, Hungund BL, Cooper TB, Tejani-Butt SM (2012): Dysfunction in fatty acid amide hydrolase is associated with depressive-like behavior in Wistar Kyoto rats. *PLoS One* 7:e36743.
- Carnevali L, Vacondio F, Rossi S, Callegari S, Macchi E, Spadoni G, *et al.* (2015): Antidepressant-like activity and cardioprotective effects of fatty acid amide hydrolase inhibitor URB694 in socially stressed Wistar Kyoto rats. *Eur Neuropsychopharmacol* 25:2157–2169.
- Du WW, Yang W, Chen Y, Wu ZK, Foster FS, Yang Z, *et al.* (2017): Foxo3 circular RNA promotes cardiac senescence by modulating multiple factors associated with stress and senescence responses. *Eur Heart J* 38:1402–1412.
- Wu N, Yuan Z, Du KY, Fang L, Lyu J, Zhang C, *et al.* (2019): Translation of yes-associated protein (YAP) was antagonized by its circular RNA via suppressing the assembly of the translation initiation machinery. *Cell Death Differ* 26:2758–2773.
- Sai J, Xiong L, Zheng J, Liu C, Lu Y, Wang G, *et al.* (2016): Protective effect of Yinhuo Miyanling Tablet on lipopolysaccharide-induced inflammation through suppression of NLRP3/caspase-1 inflammatory in human peripheral blood mononuclear cells. *Evid Based Complement Alternat Med* 2016:2758140.
- Legnini I, Di Timoteo G, Rossi F, Morlando M, Briganti F, Sthandier O, *et al.* (2017): circ-ZNF609 is a circular RNA that can be translated and functions in myogenesis. *Mol Cell* 66:22–37.e9.